Quantum Semiclass. Opt. **8** (1996) 823–836. Printed in the UK

Evolution of the vacuum Rabi peaks in a many-atom system

J Gripp and L A Orozco

Department of Physics, State University of New York, Stony Brook, NY 11794-3800, USA

Received 15 December 1995, in final form 23 April 1996

Abstract. The two peaks of the vacuum Rabi splitting behave like simple harmonic oscillators for very weak excitation. The transmission spectrum of a cavity filled with two-level atoms shows this doublet at low values of the driving intensity, but only a single peak at high values. The evolution from a doublet to a singlet is governed by the anharmonic response of the system as the driving intensity increases. The anharmonicity can grow to a point where frequency hysteresis appears in the transmission spectrum. This work investigates theoretically with a semiclassical model the transition from the doublet into the singlet. The stability of the different solutions is analysed as the parameters of atomic and cavity detuning vary. The model is extended to include the experimentally relevant transverse profile of the cavity mode as well as the standing wave structure of the field.

1. Introduction

The study of the spectroscopy of a collection of two-level atoms coupled to a single mode of the electromagnetic field has a long and distinguished history in quantum optics [1]. The pioneering work of Sánchez Mondragón *et al* [2] analysed the Jaynes–Cummings model [3] where a single atom couples to a single mode of the electromagnetic field. They revealed the composite structure of the system and the importance of the coupling between the atom and the field. They calculated the spectrum and termed the double peak present for very weak excitation the vacuum Rabi splitting. It was soon realized that the structure is indeed present even when N atoms couple to a single mode of the electromagnetic field [4], with the enhancement in the coupling constant due to the coherent interaction of all of them. In the presence of dissipation caused by the finite transmission of the cavity and by the spontaneous emission of the atom, the double-peak structure can still survive under conditions very similar to those established by Lamb [5] in his work on level crossings. The conditions amount to an impedance matching. First, the difference between the two dissipation rates has to be smaller than the coupling rate. Second, the average of the dissipation rates has to be smaller than the coupling rate, to allow multiple exchange of excitation inside the system before the energy decays away.

Over the last two decades, the investigations of the fundamental interaction of two-level atoms coupled to a single mode have taken two main paths. The first, dedicated to the active system, produced a vast literature examining a single excited two-level atom interacting with the mode of a resonator either in the microwave regime (see, for example, the review paper by Raithel *et al* [6]) or in the visible [7]. The second path studies the passive system, where the atoms are in the ground state and the cavity mode is externally excited. The latter is the canonical model of optical bistability [8].

1355-5111/96/040823+14$19.50

The experiments of Kaluzny *et al* [9] with Rydberg atoms in microwave cavities in superradiance showed the exchange of excitation between the electromagnetic mode and the collection of two-level atoms. Focusing on the passive system in the optical domain, Brecha *et al* [10] studied the transient response of a collection of two-level atoms in a single-mode optical cavity to very weak step excitation. The exchange of energy between the cavity and the atoms produced oscillations in the transmitted field at the coupling frequency. Later, different experimental groups began to study the low intensity spectrum of the same system, either by using sideband techniques [11, 12] or by measuring the transmission of the cavity as a function of the excitation frequency [13].

It was recognized early in the discussion of the passive problem that the underlying mechanism in the limit of very weak excitation could be described by a model of two coupled harmonic oscillators. Carmichael [14] formalized this idea using the Schwinger representation of a two-level atom in terms of two boson operators, the first representing the creation (annihilation) of an excited state and the second the creation (annihilation) of a ground state. Of the three harmonic oscillators present in the problem (one for the field and two for the atom), only two oscillators are necessary: one for the field and one for the excited state of the atom. The validity of this approach breaks down as soon as the excited state contains an appreciable population. In the weak-field limit the results derived from the quantum mechanical and semiclassical approaches are the same because the physics is contained in a pair of coupled harmonic oscillators.

This paper presents a semiclassical analysis of the passive system of N two-level atoms coupled to a single mode of the electromagnetic field. We go beyond the weak excitation limit and take into account the experimentally relevant transverse profile of the mode and the standing waves of the Fabry–Perot cavity. This permits us to make quantitative predictions for on-going experiments. The review chapter by Carmichael *et al* [15] stated the existence of bistable behaviour in the transmitted intensity of a driven cavity. They study a full quantum model and only show semiclassical calculations to contrast the different qualitative predictions of the two (see also Tian and Carmichael [16]). We were motivated by this difference to investigate further the problem of the transmitted spectrum of a driven cavity filled with N two-level atoms. There is a distinct evolution of the transmitted spectrum that requires a careful analysis with an experimentally appropriate model. The presence of a Gaussian transverse profile qualitatively changes the phenomenology predicted with plane waves [17]. This paper shows the results of an investigation on the evolution of the vacuum Rabi peaks as the parameters of the system vary. We map the position of the peaks as the excitation of the system increases. We allow for a possible detuning between the atomic and the cavity resonance frequencies. The explored values of the rates for cavity decay, atomic decay and single-atom coupling are kept within the experimentally relevant range [18], where all of them are of the same order. This defines the intermediate regime of cavity quantum electrodynamics.

The relevance of this problem goes beyond the field of quantum optics. Recent observations in semiconductor microcavities reveal similar phenomena. The vacuum Rabi doublet has been studied experimentally [19–21] using excitons in cavities. Although the transmitted spectrum at low intensity shows the same vacuum Rabi splitting, the underlying physical mechanisms in semiconductors and two-level atoms differ significantly. The bosonic character of the excitons and the way they may couple to each other, changes the spectrum qualitatively from the one obtained with two-level atoms.

The paper is organized as follows. In section 2 we present the semiclassical model of the system with plane waves. Section 3 is dedicated to analytical results obtained with the model under certain limits in order to gain physical understanding. Section 4 presents numerical

results of the model in the presence of atom–cavity detuning. Section 5 generalizes the model to include the experimentally relevant transverse profile of the electromagnetic field of the cavity as well as the standing waves of the Fabry–Perot cavity. Section 6 summarizes the work and presents the conclusions.

2. Model

We start with the Maxwell–Bloch equations for the atoms–cavity system, following the literature in optical bistability [8]. We work with a collection of N radiatively broadened two-level atoms interacting with a single plane-wave travelling mode of the electromagnetic field. We take the uniform field limit [8] where the absorption by the atoms and the transmission of the mirrors go to zero, while their ratio remains constant and arbitrary. The decay rate of the atoms is characterized by $\gamma_\perp$ and the cavity field decays with a rate κ. The dipole coupling between N two-level atoms and the cavity mode is $g\sqrt{N}$, where $g = (\mu^2\omega/2\hbar\epsilon_0 V)^{1/2}$; μ is the transition-dipole moment of the atom, ω the resonance frequency of both atoms and cavity and V the cavity mode volume. The cooperativity parameter of optical bistability C is related to the dipole coupling by

$$C = \frac{g^2 N}{2\gamma_\perp \kappa} \,. \tag{1}$$

The cavity and atomic detunings are given by Θ and Δ, respectively

$$\Theta = \frac{\omega_c - \omega_l}{\kappa} \tag{2}$$

$$\Delta = \frac{\omega_a - \omega_l}{\gamma_\perp} \tag{3}$$

where ω_c, ω_l and ω_a are the frequencies of the cavity resonance, excitation source and atomic resonance. The detunings are measured in units of the cavity half width κ and the atomic resonance half width $\gamma_\perp$. We only consider radiative decay in the model, so $2\gamma_\perp = \gamma_\parallel$, with $\gamma_\parallel = \tau^{-1}$, where τ is the radiative lifetime of the atomic transition. Then for a ring cavity with plane waves the Maxwell–Bloch equations have the following form:

$$\frac{\mathrm{d}x}{\mathrm{d}t} = -\kappa[(1 + \mathrm{i}\Theta)x - y + 2Cp] \tag{4a}$$

$$\frac{\mathrm{d}p}{\mathrm{d}t} = -\gamma_\perp[(1 + \mathrm{i}\Delta)p - xm] \tag{4b}$$

$$\frac{\mathrm{d}m}{\mathrm{d}t} = -\gamma_\parallel\left[m - 1 + \tfrac{1}{2}(xp^* + x^*p)\right] \tag{4c}$$

where y is the intracavity field without atoms, normalized to the square root of the saturation intensity of the atomic transition. It is proportional to the driving input field that excites the system through the field enhancement factor of the cavity. x is the intracavity field in the presence of atoms, normalized to the square root of the saturation intensity of the atomic transition. It is proportional to the output field through the transmission properties of the exit mirror. p is the scaled atomic polarization and m the scaled population difference between atoms in the ground state and in the excited state. The intensities associated with the driving and transmitted fields are $Y = |y|^2$ and $X = |x|^2$.

The steady state solution to the Maxwell–Bloch equations 4(a–c) leads to the state equation of optical bistability [8]:

$$y = x\left(1 + \frac{2C}{1 + |x|^2 + \Delta^2}\right) + \mathrm{i}x\left(\Theta - \frac{2C\Delta}{1 + |x|^2 + \Delta^2}\right). \tag{5}$$

We define a detuning Ω of the excitation frequency, which in the resonant case ($\omega_a = \omega_c$) is

$$\Omega = \gamma_\perp \Delta = \kappa \Theta \ . \tag{6}$$

Using equations (1) and (6) we derive from (5) an implicit expression for the transmitted field

$$x = y \frac{\kappa(\gamma_\perp + \mathrm{i}\Omega)}{(\kappa + \mathrm{i}\Omega)(\gamma_\perp + \mathrm{i}\Omega) + g^2 N/(1 + \gamma_\perp^2 |x|^2/(\gamma_\perp^2 + \Omega^2))} \ . \tag{7}$$

The transmission can be written in the following form to stress the two normal modes present in the low intensity regime:

$$\left|\frac{x}{y}\right|^2 = \left|\frac{A}{\mathrm{i}\Omega + \Omega_1} + \frac{B}{\mathrm{i}\Omega + \Omega_2}\right|^2 \tag{8}$$

where

$$A = \kappa \frac{\gamma_\perp + \Omega_1}{\Omega_1 - \Omega_2} \tag{9}$$

$$B = \kappa \frac{\gamma_\perp + \Omega_2}{\Omega_2 - \Omega_1} \tag{10}$$

and

$$\Omega_{1,2} = -\frac{\kappa + \gamma_\perp}{2} \pm \mathrm{i}\sqrt{-\left(\frac{\kappa - \gamma_\perp}{2}\right)^2 + \frac{g^2 N}{1 + \gamma_\perp^2 |x|^2/(\gamma_\perp^2 + \Omega^2)}} \ . \tag{11}$$

In the limit of very low excitation, $|x|^2 \ll 1$, the system behaves like two coupled harmonic oscillators and $\Omega_{1,2}$ are the eigenvalues of the linearized Maxwell–Bloch equations. In this limit, it is convenient to define the vacuum Rabi frequency as

$$\Omega_{VR} = g\sqrt{N} \ . \tag{12}$$

Note that in order to have an imaginary part in the eigenvalues $\Omega_{1,2}$ from (11), the difference between the two decay rates κ and $\gamma_\perp$ should be small compared to the vacuum Rabi frequency. To avoid overdamping in the system, the average of the two decay rates has to be smaller than the vacuum Rabi frequency.

3. Analytical results

To study the transmission, we present in figure 1 the transmitted spectrum for three values of the incident intensity Y. We normalize the spectra to the values X_{crit}, Y_{crit} at the point where the system jumps down from the upper branch of the on-resonance hysteresis curve. In the low intensity regime the structure of (8) shows two harmonic oscillators. They correspond to the normal modes of the atoms–cavity system when the excitation is very small. As the intensity increases, the excitation $|x|^2$ changes the eigenvalues given in the low intensity limit of (11). The peaks move toward the on-resonance centre and deform into a multivalued shape before they meet. The system exhibits frequency hysteresis in this regime.

We present in the remainder of this section an approximation with analytical results that helps us to understand the physical origin of the phenomenon described. We follow the work of Zhu *et al* [13] in recognizing from (5) the possibility of a phase difference between the driving field y and the intracavity field x for a weak field. Although a zero phase is not

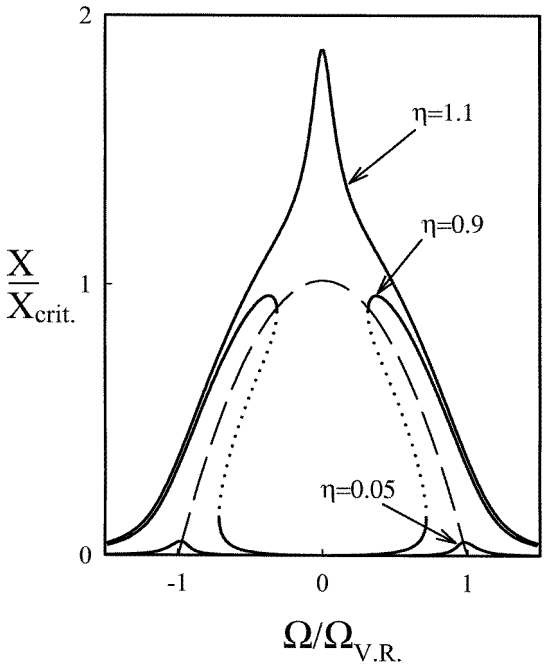

Figure 1. Transmitted intensity of the atoms–cavity system as a function of excitation frequency Ω. The curves correspond to different driving intensities $\eta = Y/Y_{crit}$. The broken curve follows the condition for zero-phase shift between the input and output fields. We show only the features reached by scanning Ω from below to above atomic resonance. The dotted curve corresponds to an unstable state. ($\Omega_{VR} =$ 35.5 MHz, $\kappa = \gamma_\perp = 3.0$ MHz, $X_{crit} = 137$, $Y_{crit} = 556$.)

a sufficient condition for a peak, a nonzero phase difference leads to destructive interference and decreases the transmission. We generalize this condition for arbitrary intensities.

The broken curve in figure 1 is obtained by demanding a phase difference of zero between the driving and the intracavity field. It is the skeleton curve for the evolving peaks

$$\Theta = \frac{2C\Delta}{1 + |x|^2 + \Delta^2}\,. \tag{13}$$

The solution $\Theta = \Delta = 0$ gives a peak only for high intensity. The condition imposed by (13) becomes more transparent in the resonant case ($\omega_a = \omega_c$) when the cavity decay rate κ and the atomic decay rate $\gamma_\perp$ are equal

$$\gamma_\perp^2|x|^2 + \Omega^2 = g^2N - \gamma_\perp^2\,. \tag{14}$$

The left-hand side of (14) is the square of the generalized Rabi frequency while the right-hand side is the square of the coupling constant between N two-level atoms and a single mode of the electromagnetic field, in the limit of large N. This shows that a high transmission due to a zero-phase difference can be achieved when the frequency separation between one of the sidebands and the main peak of the Mollow spectrum matches the frequency of the coupling constant. The Mollow triplet itself is not observable in this method of probing the atoms–cavity system where one detects the transmission of the cavity as a function of driving frequency.

The zero-phase condition guides the position of the anharmonic peaks remarkably well and links their evolution to classical optics. From a purely phenomenological point of view, one can argue that the transmitted spectrum in the high intensity regime should be a singlet, since the atoms are saturated and do not affect the transmission of the system significantly. In the limit of no dissipation $\kappa \to 0, \gamma \to 0$ and $\kappa/\gamma \to$ constant, the steady state solution shrinks into the curve given by the zero-phase condition.

The transmitted spectrum is described by the steady state solutions of the Maxwell–Bloch equations. For intermediate excitation $X/X_{crit} \leqslant 1$, figure 1 shows that the steady state solution ceases to be a single-valued function of Ω. The dotted curves indicate unstable solutions according to a linear stability analysis of the steady state solutions of the Maxwell–Bloch equations. The transmission is bistable and exhibits hysteresis as the excitation frequency varies. The deformation of the harmonic oscillator into a bistable shape recalls the presence of an anharmonicity. Next we focus on the transition of the oscillator between the low intensity regime where it is harmonic, to the place where the intensity is large enough that the anharmonic oscillator presents an unstable solution. We take one of the two oscillators from (8) and, following the work in [22], expand its frequency response around the linear eigenvalue. Then we solve to first order in $|x|^2$ while still keeping the following approximations:

$$\frac{g^2N}{1+\gamma_\perp^2|x|^2/\left(\gamma_\perp^2+\Omega^2\right)} \gg \left(\frac{\kappa-\gamma_\perp}{2}\right)^2 \tag{15}$$

and

$$\frac{\gamma_\perp^2|x|^2}{\gamma_\perp^2+\Omega^2} \ll 1\,. \tag{16}$$

This produces a shift in the resonant frequency Ω_0 from the vacuum Rabi value to

$$\Omega_0 = \Omega_{VR} - \frac{g\sqrt{N}}{2\left(1+(\Omega_0/\gamma_\perp)^2\right)}|x|^2\ . \tag{17}$$

The resulting equation for the oscillator reduces to a third-order polynomial in $|x|^2$ that produces the characteristic shape of the anharmonic oscillator. The onset of hysteresis appears when the transmission curve develops a point of infinite slope. The critical values are

$$\Omega_h = \Omega_0 - \sqrt{3}\frac{\kappa+\gamma_\perp}{2} \tag{18}$$

$$|x_h|^2 = \frac{2}{\sqrt{3}}\frac{\kappa+\gamma_\perp}{\gamma_\perp^2}g\sqrt{N} \tag{19}$$

$$|y_h|^2 = \frac{8}{3\sqrt{3}}\frac{(\kappa+\gamma_\perp)^3}{\kappa^2\gamma_\perp^2}g\sqrt{N}\,. \tag{20}$$

These conditions for frequency hysteresis are different from the conditions for on-resonance intensity bistability and require smaller intensities. The point where the two oscillators merge into a single peak in figure 1 corresponds to the point where the on-resonance intensity bistability switches down. When $g\sqrt{N}$ is large compared to $\sqrt{\kappa\gamma_\perp}$, the values are

$$X_{crit} \approx \frac{g^2N}{\kappa\gamma_\perp} \tag{21}$$

$$Y_{crit} \approx 4\frac{g^2N}{\kappa\gamma_\perp}\,. \tag{22}$$

We have progressively approximated the expression for the single oscillator by higher-order expansions in the intracavity intensity $|x|^2$. This is equivalent to an expansion of the non-linear atomic polarization. The higher orders approximate quantitatively correctly the hysteresis behaviour, reproducing the threshold for the unstable part of the curve.

4. Evolution with atoms–cavity detunings

So far the transmitted spectrum has been studied when the atoms and the cavity are resonant with each other ($\omega_a = \omega_c$) and the coupling between them is at a maximum value. As they are allowed to be at different frequencies, the coupling decreases and the behaviour of the system resembles more the case of an uncoupled cavity and atoms. Here we limit the study to the semiclassical model, but point out that the case of the quantum mechanical calculation has been treated by Haroche [23]. In the weak-field limit, extensive theoretical and experimental studies have been performed by Raizen [24]. When the excitation is no longer small, a new complication appears since the steady states calculated with the transmission function given by a generalization of (8) may develop dynamical instabilities [17]. We start by analysing the eigenvalues with a detuning δ between the cavity and the atoms

$$\delta = \omega_a - \omega_c \tag{23}$$

so that now

$$\Omega = \gamma_\perp \Delta = \kappa\Theta + \delta\,. \tag{24}$$

The imaginary part of two of the eigenvalues of the atoms–cavity system are plotted in figure 2 for the case of very weak excitation, as the detuning δ changes. The figure presents an avoided crossing at the point where the atoms and the cavity are on resonance. This is the splitting due to the exchange of energy between the cavity and the atoms. When the detuning is large, the atoms and the cavity decouple and one of the eigenvalues clearly acquires the value of the detuned cavity, while the other asymptotically reaches zero, the eigenvalue related to the atoms. The dotted curves are the eigenvalues when the coupling is turned off, $g = 0$. The labels in the figure mark the eigenvalue corresponding to the cavity and to the atoms. The broken curve shows the zero-phase condition (13). The zero-phase condition has turning points for small Ω and large δ, since the phase shift introduced by

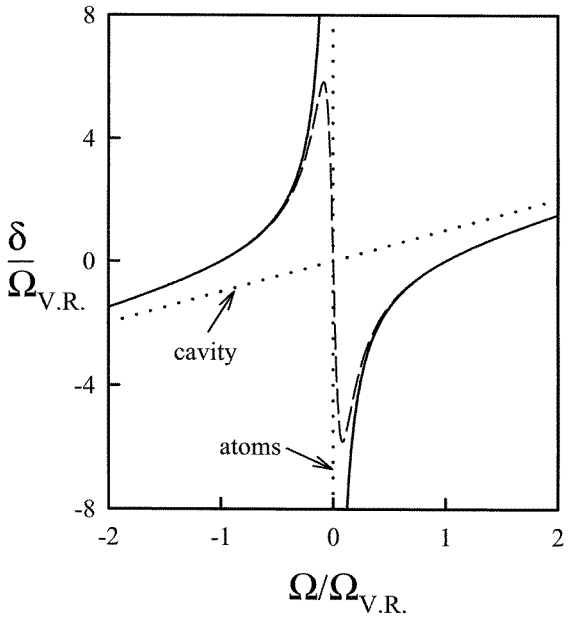

Figure 2. The full curves are the imaginary part of two of the linearized eigenvalues of the system in the limit of very low intensity $|x|^2 \ll 1$. They show an avoided crossing as the atoms–cavity detuning δ changes. The dotted curves are the eigenvalues when the interaction is turned off, $g = 0$. The two oscillators decouple as indicated in the figure. The broken curve is the zero-phase condition from (13). ($\Omega_{VR} = 35.5$ MHz, $\kappa = \gamma_\perp = 3.0$ MHz.)

the atoms is always finite and cannot compensate for arbitrarily large cavity detunings. A zero-phase difference does not imply that the transmission will have a maximum and the part of the broken curve that crosses zero is one such example. Figure 3 presents a series of transmitted spectra for very weak excitation. The asymmetry in the height of the two peaks as the detuning δ varies shows the decoupling of the two oscillators. The highest peak corresponds to the cavity resonance.

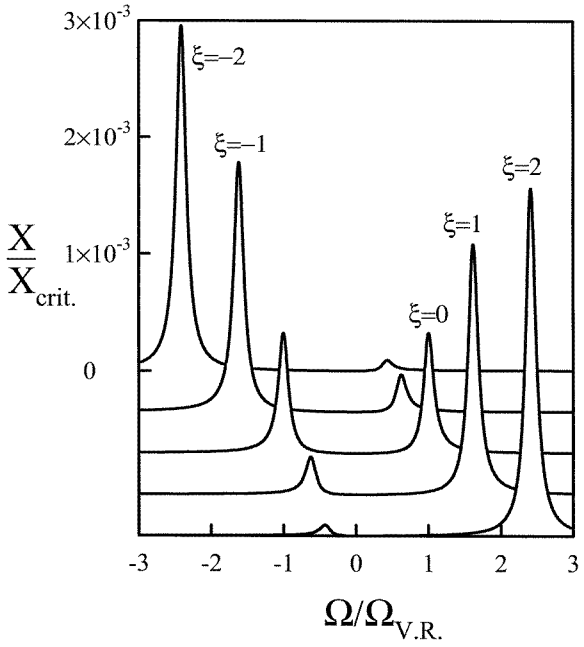

Figure 3. Transmitted spectrum for very weak excitation $Y/Y_{crit} = 0.001$ in the presence of detuning between the atoms and the cavity δ. The curves are labelled by the atoms–cavity detuning $\xi = \delta/\Omega_{VR}$. ($\Omega_{VR} = 35.5$ MHz, $\kappa = \gamma_\perp = 3.0$ MHz, $X_{crit} = 137$, $Y_{crit} = 556$.)

For the parameter space investigated in this paper, we have found, using computer calculations, that there is a direct connection between the zero-phase condition (13) and the eigenvalues of the linearized Maxwell–Bloch equations. This connection can be seen for a fixed value of x by looking at the eigenvalues as a function of Ω. The imaginary parts of two of them undergo minima in their absolute values at the frequency given by the zero-phase condition. The evolution of the system is clearly guided by this pair of eigenvalues and equivalently by the zero-phase condition. This connection can additionally be seen analytically in the linearized Maxwell–Bloch equations for the good cavity limit ($\kappa \ll \gamma_\perp$). The two eigenvalues in this limit have imaginary parts that correspond to the zero-phase condition plus a correction of higher order in $|x|^2$.

When the intracavity intensity is not small, we use the zero-phase condition from (13) and follow its behaviour as a function of intensity $|x|^2$. These plots are constructed with a fixed value of x. The three-valued solutions for certain values of δ represent three different steady states of the system, but not all of them are stable.

Figure 4 shows the modified diagram with the zero-phase condition when the intensity is not zero. The avoided crossing picture of figure 2 is lost and there is a maximum value for the detuning in the branches. As the power increases, the structure simplifies until it produces a single value representing the single peak observed in figure 1. Figure 5 maps the stability of the solutions based on a linear stability analysis of the Maxwell–Bloch equations 4(a–c). The calculation closely follows [17]. There are two possible kinds of instability, in one the system loses stability and jumps to another stable solution, the real

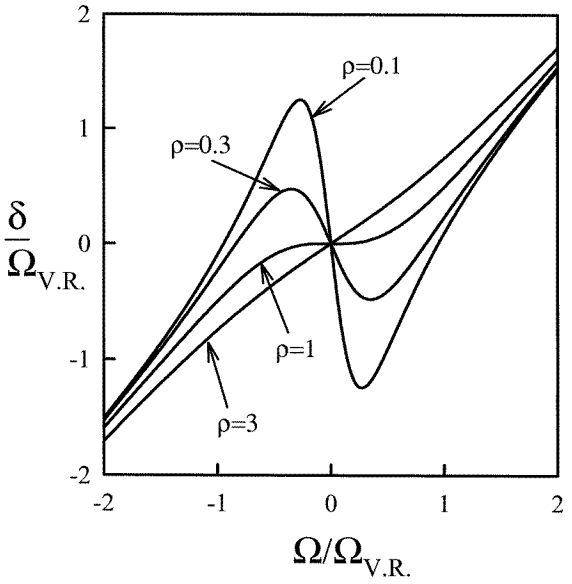

Figure 4. Evolution of the zero-phase condition in the presence of detuning between the atoms and the cavity with intermediate intensities. The curves are labelled according to the transmitted intensities $\rho = X/X_{crit}$. ($\Omega_{VR} = 35.5$ MHz, $\kappa = \gamma_\perp = 3.0$ MHz, $X_{crit} = 137$.)

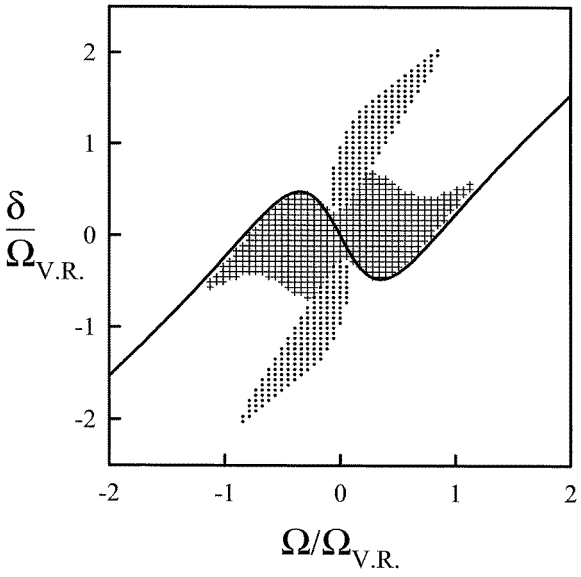

Figure 5. Linear stability analysis for the region studied in figure 4, showing the switching instability region with crosses and the dynamical instability with dots for $X/X_{crit} = 0.3$. ($\Omega_{VR} = 35.5$ MHz, $\kappa = \gamma_\perp = 3.0$ MHz, $X_{crit} = 137$.)

and imaginary parts of the eigenvalue go to zero. This is the intensity switching in optical bistability. The second possibility is where the stable solution loses stability and the system reaches a time-dependent steady state, in which the real part of the eigenvalue goes to zero, while there is a non-zero imaginary part. The new dynamical state reached is the single-mode instability of optical bistability [17].

5. Evolution with Gaussian transverse profile

The early experimental realizations in the optical regime of the simple canonical model of a collection of two-level atoms interacting with a single mode of the electromagnetic field

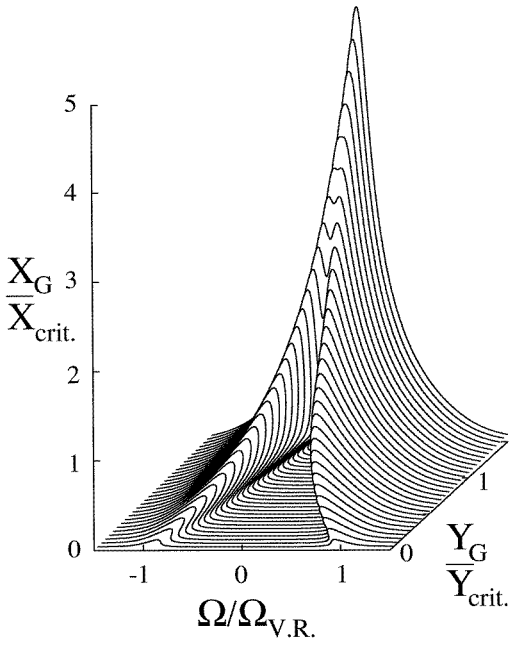

Figure 6. Transmitted spectrum as a function of the driving intensity Y_G with Gaussian transverse profile and standing waves when atoms and cavity are resonant ($\omega_a = \omega_c$). ($\Omega_{VR} = 35.5$ MHz, $\kappa = \gamma_\perp = 3.0$ MHz, $X_{crit} = 386$, $Y_{crit} = 2464$.)

[25–27] quickly demonstrated the need to include the transverse spatial profile of the cavity mode as well as the standing waves of the Fabry–Perot cavity. Quantitative comparisons between theory and experiment for the steady state response of the system achieved absolute agreement to within reported uncertainties of 10% [28]. The importance of the transverse profile was also stressed in the study of the dynamics of the states of the system [17]. Calculations of the quantum statistics [29] and squeezing spectrum [30] have also included the transverse profile. Xiao *et al* [29] stress the importance of recovering the results of the plane-wave theory whenever the intracavity field is extremely small. We have extended the results presented in the previous sections as we are interested in absolute comparisons between experiments in our laboratory and theory [18, 31]. We follow closely the treatment of [28, 32]. Starting from the Maxwell–Bloch equations and with the appropriate boundary conditions, the steady state equation relating the input and output intensities for the cavity in the presence of standing waves and a Gaussian transverse profile is

$$y_G = x_G[(1 + 2C\chi) + \mathrm{i}(\Theta - 2C\Delta\chi)] \tag{25}$$

where χ has the form

$$\chi = \frac{3}{2|x_G|^2} \ln\left[\frac{1}{2} + \frac{1}{2}\left(1 + \frac{8|x_G|^2}{3(1+\Delta^2)}\right)^{1/2}\right]. \tag{26}$$

In equation (25), y_G is the intracavity field in the absence of atoms, normalized to the square root of the saturation intensity. $|y_G|^2 = Y_G$ is related to the input intensity by the enhancement factor of the cavity. x_G is the intracavity field in the presence of atoms, normalized to the square root of the saturation intensity. $|x_G|^2 = X_G$ is related to the output intensity by the transmissivity of the exit mirror. The cooperativity C and the detunings Δ and Θ are defined by (1)–(3) in section 2.

In figure 6 we present the transmitted spectrum of a Fabry–Perot cavity operating in the TEM_{00} Gaussian mode filled with a collection of homogeneously broadened two-level

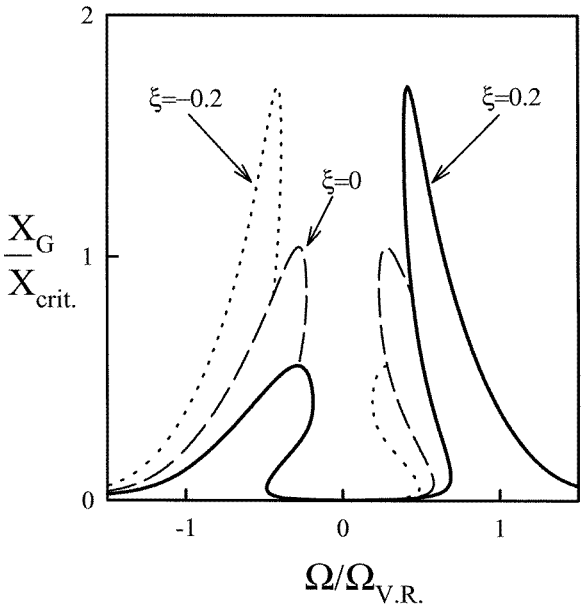

Figure 7. Modification of the transmitted spectrum in the Gaussian standing wave theory in the presence of atomic cavity detuning δ. The three traces are labelled by the atoms–cavity detuning $\xi = \delta/\Omega_{VR}$ and are taken with the same value of driving intensity $Y_G/Y_{crit} = 0.6$ ($\Omega_{VR} =$ 35.5 MHz, $\kappa = \gamma_\perp = 3.0$ MHz, $X_{crit} =$ 386, $Y_{crit} = 2464$).

atoms. The series of curves in this three-dimensional representation corresponds to a series of different values of the input intensity. The parameters chosen for this plot imply a well developed hysteresis in the input–output steady state of the system. The values of the three relevant rates g, $\gamma_\perp$ and κ fall in the intermediate regime of cavity quantum electrodynamics. For very low intensities, the two peaks of the vacuum Rabi splitting are visible. As the intensity of the driving field increases, they become anharmonic and evolve into a single peak. For very high intensities the single peak resembles the empty cavity transmission as expected when the atoms are saturated. In the presence of detuning between the atoms and the cavity, the symmetric spectra from figure 6 become asymmetric as shown in figure 7. Anharmonicity and hysteresis are still present but quantitatively modified.

Although the qualitative behaviour is similar, there are quantitative differences between the plane-wave results and those including the transverse profile. Figure 8 presents a comparison of the two models. For the resonant case of $\omega_a = \omega_c$, we focus on the positive side of the spectrum since the negative side is a mirror image of it as can be seen in figure 6. We have chosen parameters that produce the same low intensity spectrum. This means they have the same vacuum Rabi frequency Ω_{VR}. We normalize the spectra to the values X_{crit}, Y_{crit} at the point where the system jumps down from the upper branch of the on-resonance hysteresis curve. This point coincides with the place where the two anharmonic curves touch. The curves including the transverse profile show a very different evolution as a function of the driving field. The shape of the anharmonic peak is highly distorted in comparison to the equivalent one obtained with the plane-wave theory of section 2. The positions of the unstable regions causing the frequency hysteresis are quantitatively very different in terms of Ω_{VR}. In terms of the necessary relative driving intensity, the Gaussian spectrum shows earlier hysteresis than the plane wave ($\eta = 0.1$).

We have been unable to find a closed analytic expression for the zero-phase condition when the standing waves and the transverse structure of the field are included; however, a numerical calculation is possible. We demand that the driving field y_G and the transmitted field x_G have the same phase in the steady state. Then the imaginary part of (25) is set to

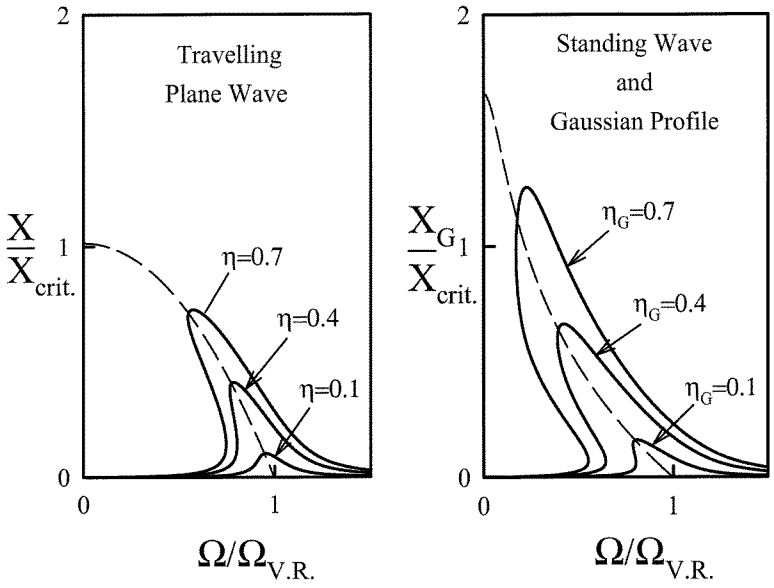

Figure 8. Comparison of the transmitted spectra between the plane-wave theory and the Gaussian standing wave theory with the atoms and cavity resonant ($\omega_a = \omega_c$). The broken curve shows the zero-phase condition. The two plots have the same value for Ω_{VR} but are normalized in the intensity by the respective switching intensities for the plane-wave model and the Gaussian standing wave model. The curves are labelled according to their values of $\eta = Y/Y_{crit}$ and $\eta_G = Y_G/Y_{crit}$. For the plane wave $X_{crit} = 137$, $Y_{crit} = 556$. For the Gaussian standing wave $X_{crit} = 386$, $Y_{crit} = 2464$ ($\Omega_{VR} = 35.5$ MHz, $\kappa = \gamma_\perp = 3.0$ MHz).

zero. In figure 8 we show with broken curves the results for both the plane-wave theory and the Gaussian with standing waves. The condition serves clearly as the skeleton curve for the evolution of the oscillators.

6. Conclusions

The study of the evolution of the vacuum Rabi sidebands has been extended in two directions. In the first one we found a connection between a zero-phase condition and the evolution of the peaks as the intensity increases. In the second one we extended the model to include the experimentally relevant condition of the Gaussian transverse profile of the electromagnetic field mode and the standing waves present when the mode is formed inside a Fabry–Perot resonator.

We have analysed the system in terms of the Maxwell–Bloch equations that are appropriate for a large number of atoms. The linearized eigenvalues of the Maxwell–Bloch equations are closely linked to the zero-phase condition. The models are semiclassical in origin and cannot provide detailed information on the underlying quantum processes. However, since the dynamical behaviour of the semiclassical and quantum systems in the regime of large numbers of atoms is governed by the same eigenvalue structure, the study of one can sometimes shed light on the other.

The evolution from a pair of simple harmonic oscillators to highly anharmonic ones is caused by the non-linear polarization of the collection of two-level atoms. As the intracavity intensity increases, the atomic transition saturates and higher-order terms of the driving

field have to be taken into account. The anharmonicity is the semiclassical counterpart of the multiphoton resonances in the energy level structure of an atom–cavity system that allow for the generation of non-classical states of the electromagnetic field in the system [33, 34].

These calculations permit the exploration of the parameter space of the atoms–cavity interaction in a systematic way. Future work includes the development of a fully quantum mechanical model and its connection with the semiclassical results.

Acknowledgments

We would like to acknowledge many helpful conversations with S L Mielke and H J Carmichael. This work was supported by the National Science Foundation under grant PHY-9321203.

References

[1] Berman P R (ed) 1994 *Cavity Quantum Electrodynamics* (San Diego, CA: Academic)
[2] Sánchez Mondragón J J, Narozhny N B and Eberly J H 1983 *Phys. Rev. Lett.* **51** 550
[3] Jaynes E T and Cummings F W 1963 *Proc. IEEE* **51** 89
[4] Agarwal G S 1984 *Phys. Rev. Lett.* **53** 1732
[5] Lamb W E Jr 1952 *Phys. Rev.* **85** 259
[6] Raithel G, Wagner C, Walther H, Narducci L M and Scully M O 1994 *Cavity Quantum Electrodynamics* ed P R Berman (San Diego, CA: Academic) p 57
[7] An K, Childs J J, Dasar R R and Feld M S 1994 *Phys. Rev. Lett.* **73** 3375
[8] Lugiato L A 1984 *Progress in Optics* vol XXI ed E Wolf (Amsterdam: North-Holland) p 69
[9] Kaluzny Y, Goy P, Gross M, Raimond J M and Haroche S 1983 *Phys. Rev. Lett.* **51** 1175
[10] Brecha R J, Orozco L A, Raizen M G, Xiao Min and Kimble H J 1995 *J. Opt. Soc. Am.* B **12** 2329
[11] Raizen M G, Thompson R J, Brecha R J, Kimble H J and Carmichael H J 1989 *Phys. Rev. Lett.* **63** 240
[12] Thompson R J, Rempe G and Kimble H J 1992 *Phys. Rev. Lett.* **68** 1132
[13] Zhu Yifu, Gauthier D J, Morin S E, Wu Qilin, Carmichael H J and Mossberg T W 1990 *Phys. Rev. Lett.* **64** 2499
[14] Carmichael H J 1986 *Phys. Rev.* A **33** 3262
[15] Carmichael H J, Tian L, Ren W and Alsing P 1994 *Cavity Quantum Electrodynamics* ed P R Berman (San Diego, CA: Academic) p 381
[16] Tian L and Carmichael H J 1992 *Quantum Electronics and Laser Science Conf.* (OSA Technical Digest Series **13**) (Washington, DC: Optical Society of America)
[17] Orozco L A, Kimble H J, Rosenberger A T, Lugiato L A, Asquini M L, Brambilla M and Narducci L M 1989 *Phys. Rev.* A **39** 1235
[18] Gripp J, Mielke S L, Orozco L A and Carmichael H J to be published
[19] Weisbuch C, Nishioka M, Ishikawa A and Arakawa Y 1992 *Phys. Rev. Lett.* **69** 3314
[20] Cao H, Jacobson J, Björk G, Pau S and Yamamoto Y 1995 *Appl. Phys. Lett.* **66** 1107
[21] Shah Jagdeep, Wang Hailin, Damen T C, Jan W Y and Cunningham J E 1995 Coherent oscillations in semiconductor microcavities *Quantum Electronics Conf.* (OSA Technical Digest Series **16**) (Washington, DC: Optical Society of America) p 228
[22] Landau L D and Lifshitz E M 1976 *Mechanics* 3rd edn (Oxford: Pergamon)
[23] Haroche S 1992 *Les Houches Summer School Session LIII: Fundamental Systems in Quantum Optics* ed J Dalibard, J M Raimond and J Zinn-Justin (Amsterdam: Elsevier) p 767
[24] Raizen M 1989 *PhD Dissertation* University of Texas at Austin, unpublished
[25] Grant D E and Kimble H J 1982 *Opt. Lett.* **7** 353
[26] Sandle W J and Gallagher A 1981 *Phys. Rev.* A **24** 2017
[27] Rosenberger A T, Orozco L A and Kimble H J 1983 *Phys. Rev.* A **28** 2569
[28] Rosenberger A T, Orozco L A, Kimble H J and Drummond P D 1991 *Phys. Rev*. A **43** 6284
[29] Xiao M, Kimble H J and Carmichael H J 1987 *Phys. Rev.* A **35** 3832
[30] Hope D M, McClelland D E and Savage C M 1990 *Phys. Rev.* A **41** 5074
[31] Gripp J, Mielke S L and Orozco L A 1995 *Phys. Rev.* A **51** 4974

[32] Drummond P D 1981 *IEEE J. Quantum Electron.* **QE-17** 301
[33] Raizen M G, Orozco L A, Xiao Min, Boyd T L and Kimble H J 1987 *Phys. Rev. Lett.* **59** 198
Orozco L A, Raizen M G, Xiao Min, Brecha R J and Kimble H J 1987 *J. Opt. Soc. Am.* B **4** 1490
[34] Hope D M, Bachor H-A, Manson P J, McClelland D E and Fisk P T H 1992 *Phys. Rev.* A **46** R1181